

## Efficient solidification of Pb<sup>2+</sup> by activated tungsten tailings and cement

Hao Cheng<sup>1</sup>, Jingzhong Kuang<sup>1,2</sup>, Luping Zhu<sup>1</sup>, Weiquan Yuan<sup>1</sup>, Zheyu Huang<sup>1</sup>, Yiqiang Yang<sup>1</sup>

<sup>1</sup> School of Resource and Environmental Engineering, Jiangxi University of Science and Technology, Ganzhou, 341000, China

<sup>2</sup> Jiangxi Key Laboratory of Mining Engineering, Ganzhou, 341000, China

Corresponding author: [kjz692@163.com](mailto:kjz692@163.com) (Jingzhong Kuang)

**Abstract:** The preparation of cementing admixture from tailings and co-solidification of Pb<sup>2+</sup> with cement is a green way to realize the resource utilization of tailings and treatment of the lead-containing wastewater. In this paper, the tungsten tailings were activated in different ways, and the mechanical properties of the tungsten tailings-cement solidified body with different activation systems and the solidification behavior of Pb<sup>2+</sup> were studied. The phase and microstructure of the hydrated product were characterized by XRD, FT-IR, SEM and EDS. The results showed that the curing effect of Pb<sup>2+</sup> was obviously different of different activation systems, and the curing effect of the solidified body of the ternary composite activation system (TCAS) was the best, second only to the pure cement system (PCS). Different activation methods have a significant impact on the mechanical properties of the solidified body. With the increase of the Pb<sup>2+</sup> content, the compressive strength of the solidified body gradually decreased, the Pb<sup>2+</sup> leaching concentration gradually increased; with the extension of the curing age, the compressive strength gradually increased, and the Pb<sup>2+</sup> leaching concentration gradually decreased. In particular, the compressive strength of the 28d solidified body was 31.43 MPa and the leaching concentration of Pb<sup>2+</sup> was only 0.38 mg/L when the Pb<sup>2+</sup> content was 5%. The phase, microstructure and EDS results of the hydration products showed that Pb<sup>2+</sup> was mainly solidified in the C-S-H gel.

**Keywords:** tungsten tailings, activation, Pb<sup>2+</sup>, solidification, C-S-H gel

### 1. Introduction

China is a major producer of tungsten (Feng et al., 2011; Peng et al., 2006), and a large number of tailings are produced in the process of mining and processing (Feng et al., 2013; Khan et al., 2012; Lee et al., 2014), the annual discharge of tungsten tailings is about 10 million tons (Liu et al., 2010). At present, the main treatment method of tungsten tailings is to store them in tailings ponds, which not only occupies a large amount of land, causes environmental pollution and waste of resources, also has potential safety hazards (Lee et al., 2012; Petrunic et al., 2006; Wang et al., 2022). The research on the comprehensive utilization of tungsten tailings resources mainly includes two aspects: One is to recover valuable minerals in tailings (Huang et al., 2022; Whitworth et al., 2022), and the other is to use tungsten tailings to prepare building materials (Alfonso et al., 2018; Choi et al., 2009; Peng et al., 2015; Zhu et al., 2022), such as glass-ceramics, ceramics, sintered bricks, mineral aggregates, etc. How to reduce environmental pollution and realize large-scale utilization of tungsten tailings is extremely urgent.

Pb<sup>2+</sup> is an important source of pollution in wastewater with a wide range of sources. Non-ferrous metal mining, lead storage batteries, electronics, metal electroplating, steel manufacturing and other industries will produce a large amount of lead-containing wastewater (Chen et al., 2021; Katsou et al., 2011). Pb<sup>2+</sup> is not degradable and can exist in the environment for a long time, causing the Pb<sup>2+</sup> content in water and soil to exceed the standard (Liu et al., 2013), and causing serious harm to human health through the food chain (EI-Eswed et al., 2017; Yuan et al., 2021). Lead-containing wastewater has always been one of the difficult problems in the field of wastewater treatment. Commonly used treatment

methods include chemical precipitation (Kumar et al., 2021), adsorption (Ravishankar et al., 2019), membrane separation (Kharraz et al., 2022), ion exchange (Pranudta et al., 2021) and bioremediation (Oliveira et al., 2022). The wastewater treatment process will produce sediments and floating objects, which contain  $Pb^{2+}$  and pathogenic microorganisms, which are difficult to treat and easily cause secondary environmental pollution (Kharraz et al., 2022). In addition, curing  $Pb^{2+}$  with curing agent is also a good treatment method. By adding a curing agent, the  $Pb^{2+}$  is fixed in the solidified body with stable properties and certain strength by physical or chemical methods, or the  $Pb^{2+}$  is converted into a chemically inactive form to form a sealing effect and prevent it from migrating and diffusing in the environment, to prevent the occurrence of secondary pollution to the greatest extent. At present, the solidification method is more applied to the treatment of heavy metal-containing sludge and fly ash and other wastes (El-eswed, 2020; Ji and Pei, 2019), with the purpose of immobilizing heavy metal ions in the solidified body with stable properties and making the mechanical properties of the solidified body meet the relevant engineering requirements.

Cement-based solidification techniques can be used to solidify  $Pb^{2+}$  in wastewater (Conner and Hoeffner, 1998). On the one hand, cement can provide an alkaline environment to promote the formation of  $Pb^{2+}$  precipitation, and on the other hand, the hydration products of cement can adsorb and encapsulate  $Pb^{2+}$  (Chen et al., 2009), so as to achieve the purpose of immobilizing lead ions. Halim et al. (2004) pointed out that  $Pb^{2+}$  was uniformly distributed in the C-S-H gel by adsorption and precipitation. Lee (2007) found that in addition to C-S-H gel,  $Pb^{2+}$  was also distributed in other hydration products. However, the traditional cement curing method has many problems (Glasser, 1997): large cement consumption, high curing cost, high energy consumption in the cement production process, and the production of a large amount of  $CO_2$  to accelerate the greenhouse effect. Every ton of Portland cement produced emits 0.85 to 1 ton of carbon dioxide into the atmosphere (Monteiro et al., 2017), and it is crucial to reduce greenhouse gas emissions from the cement industry. Therefore, finding a substitute for cement has become a new research direction. At present, there are studies that can be used as cementitious materials to replace cement, such as kaolin, fly ash and tail slag, etc. (Siddique, 2010; Tian et al., 2022; Wu et al., 2021). Ji and Pei (2020) prepared geopolymers from water treatment residues and blast furnace slag, and found that the hydration products have a good wrapping effect on  $Pb^{2+}$ ,  $Pb^{2+}$  is evenly distributed in the geopolymers, and the geopolymers can maintain strong stability. Due to the minerals in tungsten tailings are similar in structure to pozzolanic materials (Peng et al., 2015), activation and excitation treatment can make them amorphous and have certain gelling activity, which can be used to prepare auxiliary gelling materials. Therefore, tungsten tailings synergize with cement to solidify  $Pb^{2+}$  is a potential way to solve the problem of tungsten tailings stockpiling and pollution,  $CO_2$  emissions and lead-containing wastewater.

In this paper, tungsten tailings were treated in different activation ways, and highly soluble  $Pb(NO_3)_2$  was selected as the source of  $Pb^{2+}$  to increase the content of  $Pb^{2+}$  in the raw materials, aiming to simulate lead-containing wastewater. The solidification behaviour and mechanism of  $Pb^{2+}$  in different systems of tungsten tailings-cement solidified body were studied, and the possibility of treating lead-containing wastewater by this method was evaluated. This method can treat both waste tungsten tail and lead-containing wastewater, which is the innovation of this study.

## 2. Materials and methods

### 2.1. Experimental materials

The tailings used in this experiment were taken from a scheelite tailings in Jiujiang, Jiangxi Province. The chemical composition is shown in Table 1, mainly  $SiO_2$ ,  $Fe_2O_3$  and  $CaO$ . The XRD phase analysis results of the tailings are shown in Fig. 1, mainly quartz, and a small amount of calcite, fluorite, diopside, etc.

Table 1 XRF results of element content (%) in tungsten tailings

$SiO_2$	$Al_2O_3$	$Fe_2O_3$	$K_2O$	$CaO$	$BiO$	$Na_2O$	$TiO_2$
38.48	2.01	14.59	0.69	16.58	0.05	0.87	0.22
$MnO$	$SO_3$	$P_2O_5$	$Rb_2O$	$ZnO$	$CuO$	$WO_3$	$PbO$
0.72	11.36	0.01	0.01	0.17	0.29	0.63	0.03

The cement used in the test was ordinary 42.5 Portland cement, the chemicals gypsum (G1), triethanolamine (T1), diethylene glycol (D1) and lead nitrate were all analytically pure, and the water was deionized water.

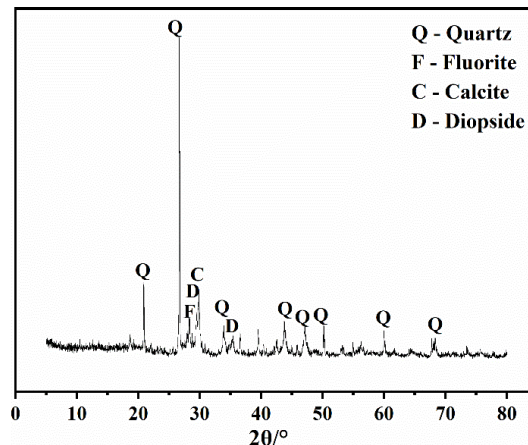


Fig. 1. XRD pattern of tungsten tailings

## 2.2. Experimental process

### 2.2.1. Activation of tungsten tailings

3.5 kg tailings were added into SM-500 ball mill for 30 mins mechanical grinding activation, during the grinding process, added a certain amount of unary activator T1, binary composite activator T1 + D1 and ternary composite activator T1 + D1 + C1 for mechanical chemical composite activation (MCCA), four required tungsten tailings were obtained.

### 2.2.2. Preparation of solidified body

Firstly,  $Pb^{2+}$  ( $Pb(NO_3)_2$ ) containing solutions with different mass fractions were prepared, then referred to GB/T 17671-1999 (ISO method), 315g of cement, 135g of activated tailings (tailings accounted for 30% of the total weight of solids) were weighed and mixed them with prepared  $Pb^{2+}$  solution to prepare  $40 \times 40 \times 40$  mm shaped solidified body with a water cement ratio of 0.4. Three samples were made for each formula, and were demoulded after curing for 24h, and then cured for 3d, 7d and 28d in the standard curing box. The compressive strength of solidified body under different curing time was measured.

### 2.2.3. $Pb^{2+}$ leaching

The HJ/T 299-2007 nitric acid sulfuric acid method was used to leach  $Pb^{2+}$  in the tungsten tailings-cement solidified body. Firstly, an appropriate amount of sample was weighed and put it in the centrifuge tube, then the leaching liquid with a liquid-solid ratio of 10:1 was added into the tube. The mass ratio of concentrated sulfuric acid and concentrated nitric acid in the leaching liquid was 2:1, deionized water was added to prepare the solution. After turning and shaking, the solution was filtered with a microporous filter membrane to obtain the leaching solution. Finally, the leaching concentration of  $Pb^{2+}$  was measured and the data were obtained.

## 2.3. Testing and Characterization methods

The specific surface area and particle gradation of tungsten tailings were tested by Omega LS908 (A) laser particle size analyzer. The compressive strength of the solidified body of different conditions were tested by a YES-2000D pressure tester. The ion concentration of the leachate was tested with a PQ9000 Inductively Coupled Plasma Mass Spectrometer (ICP-MS). The phase analysis of the solidified body was carried out by DX-2700 X-ray diffractometer. Structural analysis of the solidified body was performed by a Perkin Elmer Spectrum Two N-type Fourier transform near-infrared spectrometer. MLA650F field emission scanning electron microscope (FEI, USA) and energy spectrometer (Bruker,

Germany) were used to observe the microscopic morphology and element content of hydration products of solidified body under different conditions.

### 3. Results and discussion

#### 3.1. Effect of cement on solidification behaviour of $Pb^{2+}$

Fig. 2 shows the effect of cement paste on the solidification behaviour of  $Pb^{2+}$  under different curing ages. The  $Pb^{2+}$  leaching concentration and leaching rate in the leaching solution of the cement paste is shown in Fig. 2(a). 2%  $Pb^{2+}$  was added into ordinary Portland cement, after curing for 3d, the  $Pb^{2+}$  leaching rate in the leaching solution was 0.035%. With the increase of curing age, the hydration reaction of cement was gradually completed, and the curing effect of  $Pb^{2+}$  was getting better. After curing for 28d, the concentration of  $Pb^{2+}$  in the leaching solution was only 0.06 mg/L, the leaching rate of  $Pb^{2+}$  was only 0.0102%, and the curing efficiency of  $Pb^{2+}$  reached more than 99.9%.

The compressive strength of the cement paste solidified body is shown in Fig. 2(b). After adding  $Pb^{2+}$ , the compressive strength of the cement solidified body was lower than that without  $Pb^{2+}$ . Because the incorporated  $Pb^{2+}$  is easy to combine with  $OH^-$  in the alkaline environment of the cement to form an amorphous lead hydroxide precipitate, which adheres to the surface of the partially hydrated cement particles, thereby hindering the further hydration reaction of the cement (Chen et al., 2009), and reducing the compressive strength of the solidified body. After 28d of curing, the compressive strength of the solidified body was 43.55 MPa, which is slightly lower than that of the pure cement solidified body was 49.87 MPa. But it also meets the strength level specified in the Chinese standards (GB175-2007), it can play a great curing effect on  $Pb^{2+}$ .

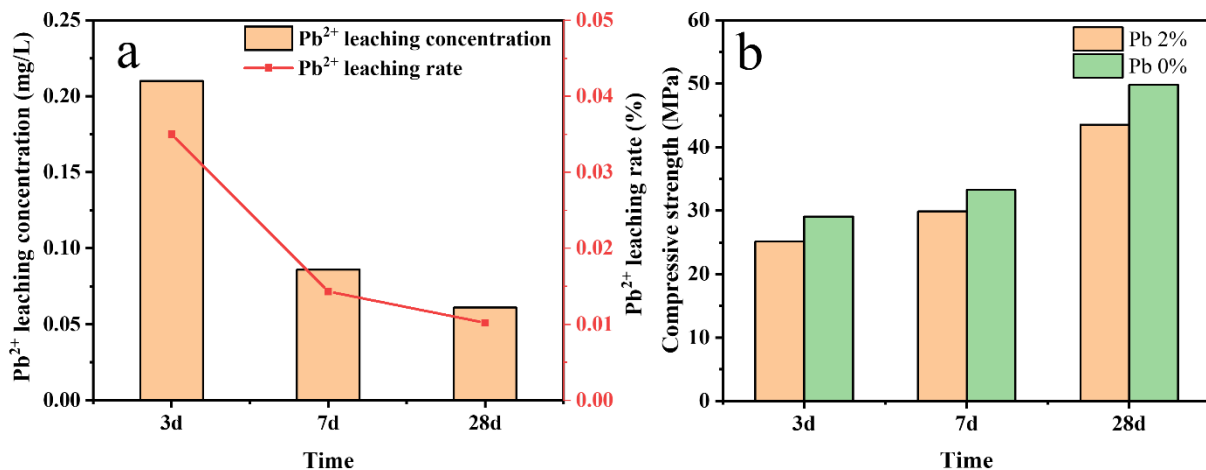


Fig. 2. Effect of cement paste on the solidification behaviour of  $Pb^{2+}$  at different curing ages (a- $Pb^{2+}$  leaching concentration and leaching rate; b-compressive strength of solidified body)

#### 3.2. Effects of different activation modes of tungsten tailings-cement solidified body on solidification behaviour of $Pb^{2+}$

When the mass fraction of  $Pb^{2+}$  was 2%, the effect of the solidified body made of cement and tungsten tailings after activation in different ways on the leaching of  $Pb^{2+}$  is shown in Fig. 3(a, b). Comparing Fig. 2(a), it could be seen that under the same conditions, when the same mass of tungsten tailings activated in different ways were mixed into the cement, the leaching rate of  $Pb^{2+}$  in each system increased, and the curing effect was not as good as that of PCS. Moreover, the leaching rate of  $Pb^{2+}$  varied with the activation methods of tungsten tailings. Compared with the MAS, the leaching rate of  $Pb^{2+}$  in the curing system of tungsten tailings after mechanical-chemical composite activation (MCCA) was lower. And after 28d of curing, the leaching concentration of  $Pb^{2+}$  in the TCAS was only 0.10 mg/L, the leaching concentration of  $Pb^{2+}$  is far lower than the upper limit of 5 mg/L specified in the Chinese standards for hazardous wastes-identification for extraction toxicity (GB5085.3-2007).

Fig. 3(c) shows the compressive strength of the solidified body under different systems, and the compressive strength was lower than that of the pure cement solidified body (Fig. 2(b)). This is because

the content of active silicon and aluminum in tungsten tailings is relatively low (Peng et al., 2015), which is not as high as that of cement. Replacing part of cement with tungsten tailings would reduce the content of active ingredients, which was not conducive to the hydration reaction of cement, resulting in a decrease in the content of hydration products, thus reducing the compressive strength of the solidified body. The compressive strength of the solidified body of the MCCA was higher than that of the MAS, and the compressive strength of the solidified body under the TCAS was the highest. With the progress of the reaction, the degree of hydration continued to deepen, and the compressive strength of the solidified body of the TCAS reached 36.26 MPa after curing for 28d. The results show that the higher the compressive strength of the solidified body, the better the curing effect of  $Pb^{2+}$  can be to a certain extent.

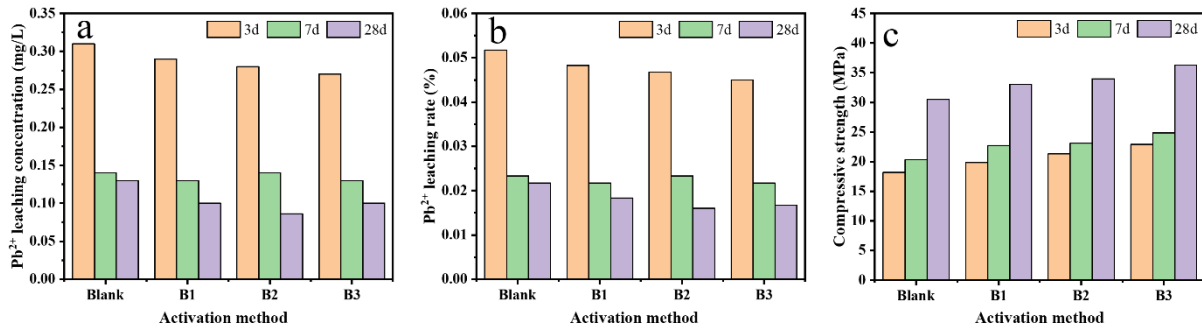


Fig. 3. Effect of different activation methods of tungsten tailings on the solidification behaviour of  $Pb^{2+}$ . a: leaching concentration of  $Pb^{2+}$ ; b: leaching rate of  $Pb^{2+}$ ; c: compressive strength of solidified body (Blank-mechanical activation system (MAS), B1-unary composite activation system (UCVS), B2-binary composite activation system (BCAS), B3-ternary composite activation system (TCAS))

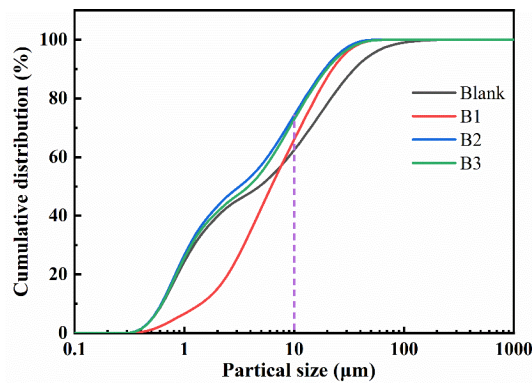


Fig. 4. Particle size distribution of tungsten tailings with different activation methods (Blank-MAS, B1-UCVS, B2-BCAS, B3-TCAS)

Activated tungsten tailings can effectively improve the particle size distribution of minerals, increase the specific surface area of the particles and increase the active sites on the surface of the particles, so that the tungsten tailings contain active  $SiO_2$ , which can participate in the hydration reaction. It can react with  $Ca(OH)_2$ , the hydrated product of cement, to form compact C-S-H gel, thus improving the compressive strength of the solidified body (Peng et al., 2015). Studies have shown (Koroglu et al., 2021) that the particle size less than  $30 \mu m$  in the cement admixture plays a positive role in improving the strength of the solidified body, and the particle size less than  $10 \mu m$  has the most obvious effect on the strength. In addition, the leaching amount of  $Pb^{2+}$  is larger under the condition of large particle size (more than  $10 \mu m$ ) (Huang et al., 2020), which is because the leaching specific surface area of large particles is small, and the leaching speed of alkali in cement-based materials in coarse particles is slow, so the pH of the solution was kept lower, making the leaching of  $Pb^{2+}$  easier. It can be seen from the particle size distribution of tungsten tailings in Fig. 4 that for tungsten tailings activated in different ways, the yields of particle sizes less than  $10 \mu m$  in the tailings are different. The results show that the tailings of MAS, the effective particle size of the particle size less than  $10 \mu m$  accounted for 62.12%. The effective particle yield of tailings of MCCA was higher than that of MAS, and the yield of BCAS and

TCAS was higher than 70%. In addition, the specific surface areas of the tailings of four different systems of MAS, UCAS, BCAS and TCAS were 647 m<sup>2</sup>/kg, 936 m<sup>2</sup>/kg, 1086 m<sup>2</sup>/kg and 1113 m<sup>2</sup>/kg, respectively. This was because the addition of chemical activators during the tailings grinding process could aggravate the structural changes inside the particles (Peng et al., 2015), most of the coarse tailings are converted into fine particles, which increases the specific surface area of the particles and helps the particles to participate in the hydration reaction, forming a hydration product, which is finally reflected in the compressive strength of the solidified body.

### 3.3. Effect of Pb<sup>2+</sup> content on curing Pb<sup>2+</sup> in solidified body

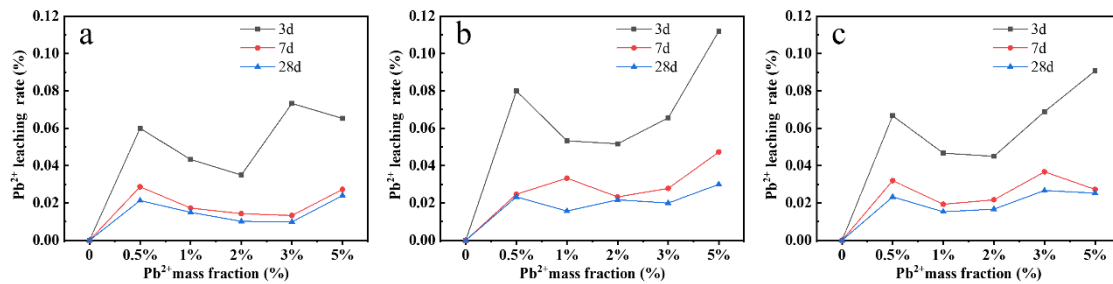


Fig. 5. Effect of Pb<sup>2+</sup> content on leaching rate of Pb<sup>2+</sup> from the solidified body (a-PCS; b-MAS; c-TCAS)

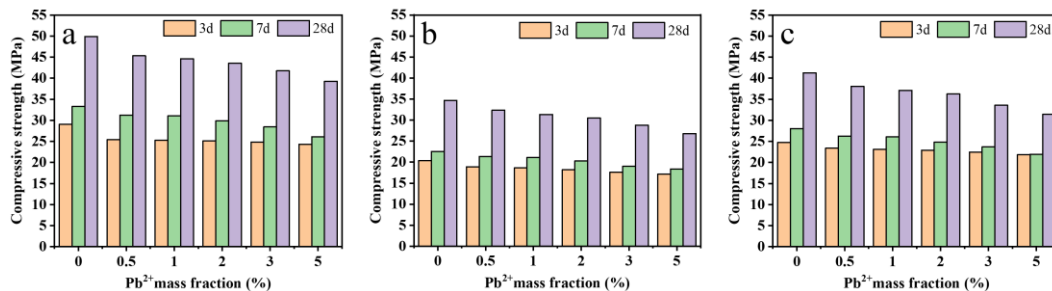


Fig. 6. Effect of Pb<sup>2+</sup> content on the compressive strength of the solidified body (a-PCS; b-MAS; c-TCAS)

Fig. 5 shows the effect of Pb<sup>2+</sup> content on the leaching of Pb<sup>2+</sup> from the solidified body of different systems. It could be seen from the figure that the rate of Pb<sup>2+</sup> leached from the PCS was lower than that of the tungsten tailings-cement activation system, and as the content of Pb<sup>2+</sup> increased from 0.5% to 5%, the leaching rate of Pb<sup>2+</sup> gradually increased. When the content of Pb<sup>2+</sup> was 2%, the leaching rate of Pb<sup>2+</sup> of PCS after hydration for 28d was only 0.0102%, that of TCAS was 0.0167%, and that of MAS was 0.0217%. When the Pb<sup>2+</sup> content was more than 3%, firstly it would react with the alkaline substances in the cement system and consume a part of OH<sup>-</sup>, since the Pb(NO<sub>3</sub>)<sub>2</sub> solution was acidic, which would hinder the cement hydration process and reduce the hydration products. Therefore, the leaching rate of Pb<sup>2+</sup> was higher in the early stage of hydration. However, with the progress of the reaction, the degree of hydration deepened, and the leaching rate of Pb<sup>2+</sup> in the solidified body decreased significantly after curing for 28d, and the leaching concentration did not exceed 0.50 mg/L, which was far lower than the upper limit of 5 mg/L specified in the Chinese standards for hazardous wastes-identification for extraction toxicity (GB5085.3-2007). The leaching results show that the solidified body prepared by activated tungsten tailings and cement can effectively immobilize Pb<sup>2+</sup>.

The effect of Pb<sup>2+</sup> content on the compressive strength of the solidified body is shown in Fig. 6. As Pb<sup>2+</sup> content increased from 0.5% to 5%, the compressive strength of the solidified body of each system gradually decreased. When Pb<sup>2+</sup> content reached 5%, the compressive strength of the solidified body of each system after curing for 28 d was 39.26 MPa, 26.77 MPa and 31.43 MPa, which was significantly lower than 49.87 MPa, 34.69 MPa and 41.26 MPa while Pb<sup>2+</sup> was not added, and the strength loss rate was 21.28%, 22.83% and 23.82% respectively. The main reason was that with the addition of Pb<sup>2+</sup>, the progress of the hydration reaction was inhibited to a certain extent (Chen et al., 2009), resulting in a decrease in the output of hydration products, which had an impact on the stability of the internal

structure of the solidified body, and ultimately manifested in the decrease in the compressive strength of the solidified body.

### 3.4. Analysis of the solidification mechanism of $Pb^{2+}$

Comparing the hydration products of the solidified bodies of different tungsten tailings-cement systems, it could be found from the XRD diagram in Fig. 7 that the main phases of the cement paste were hydration products  $Ca(OH)_2$  and AFt, and unhydrated particles  $C_2S$ ,  $C_3S$  and  $SiO_2$  for curing 3 d. In addition, the amorphous calcium silicate hydrate (C-S-H gel) was difficult to detect, and no corresponding characteristic peaks were found in the diffraction pattern. After adding tailings, the main phase in the solidified body did not change, but the diffraction peaks of unhydrated particles  $C_2S$ ,  $C_3S$  and  $SiO_2$  were slightly enhanced, and the intensity of AFt and  $Ca(OH)_2$  diffraction peaks decreased. The H-O-H bending vibration peaks of structural water at  $3440\text{ cm}^{-1}$  and  $1639\text{ cm}^{-1}$  (Mollah et al., 2000) for the solidified body of the activated system have little changed; the O-H vibration peak of  $Ca(OH)_2$  at  $3644\text{ cm}^{-1}$  (Mollah et al., 2000) and the S-O stretching vibration peak of AFt at  $1114\text{ cm}^{-1}$  were shifted to a lower wave number than that of the PCS; the stretching vibration peak of the Si-O bond shifted from  $999\text{ cm}^{-1}$  to  $996\text{ cm}^{-1}$ , and the wave number of the bending vibration peak of the Si-O bond at  $469\text{ cm}^{-1}$  reduced to  $465\text{ cm}^{-1}$ , so it was difficult for the Si-O bond to polymerize to form the Si-O-Si bond (Hu et al., 2020). It indicated that the content of AFt and  $Ca(OH)_2$  was low, the formation process of C-S-H gel was inhibited, and the degree of hydration was low. At this time, the strength of the solidified body was affected, and the curing effect of  $Pb^{2+}$  was not as good as that of PCS. As shown in the SEM image, in the PCS, some flaky  $Ca(OH)_2$  and needle-like AFt could be clearly seen in the early stage of hydration, and the hydration products are cemented with each other to form a stable network structure. However, limited by the age of hydration, there were still areas not participating in the reaction. In the activation system, most of the regions were not involved in the reaction, and the content of hydration products was less, and a few fine needle-like AFt and flake  $Ca(OH)_2$  could be seen, the network structure voids formed between them were large, and the hydration degree was not as good as that of the PCS. It was shown that the compactness of the solidified body was low, the compressive strength was insufficient, so the leaching concentration of  $Pb^{2+}$  was relatively high, which correspond to Fig. 3.

The analysis of the hydration product of the solidified body curing for 28d is shown in Fig. 8. Compared with curing for 3d, its main phase unchanged, the peaks of  $C_2S$  and  $C_3S$  decreased obviously, the intensity of  $Ca(OH)_2$  diffraction peaks decreased, and the stretching vibration peaks of O-H and Si-O bonds of hydration products were shifted to a higher wave number. This indicated that with the

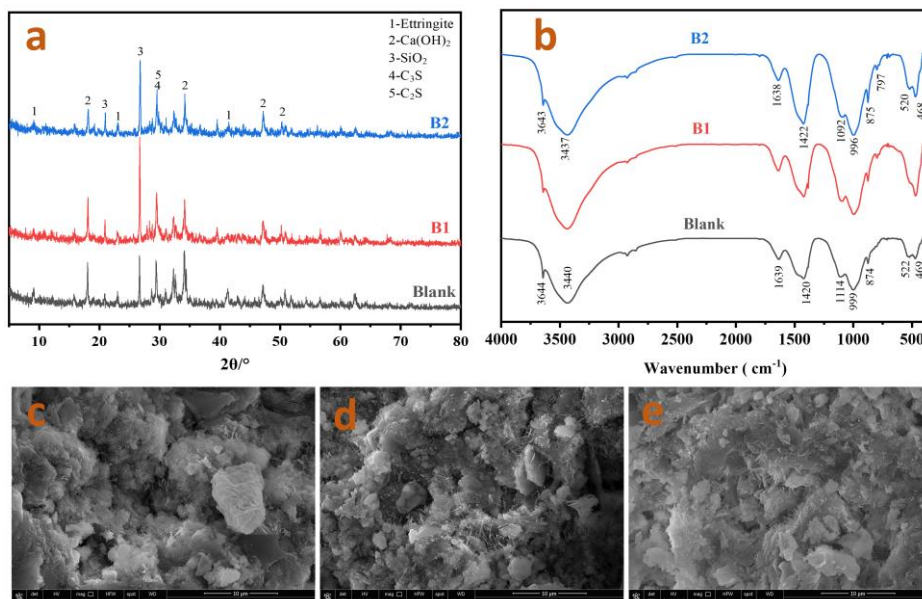


Fig. 7. Analysis of hydration products of different tungsten tailings cement system solidified bodies mixed with  $Pb^{2+}$  for 3d. (a-XRD of the solidified body; b-FT-IR of the solidified body; c-e are the SEM images of the solidified body of Blank, B1 and B2; Blank-PCS, B1-MAS, B2-TCAS)

extension of curing age of the solidified body, its hydration degree also increased, and  $\text{Ca}(\text{OH})_2$  could react with active  $\text{SiO}_2$  in tailings to form hydrated calcium silicate (Peng et al., 2015). With the progress of the reaction, the difference between the MAS and the PCS was more obvious, the degree of hydration and the content of hydration products of the MAS were far inferior to the PCS, while the TCAS was better than the MAS. It could be seen from the SEM image that with the progress of the hydration reaction, the amount of amorphous C-S-H gel in the PCS and the TCAS increased, the size of Aft increased significantly, and the voids between the reactants decreased. A dense network structure was formed, which was the main reason for the excellent mechanical properties of the solidified body. The C-S-H gel developed from an initial fibrous to a network structure (Ji et al., 2021), and with the increase of the density of the solidified body, it eventually becomes a flower-like structure. The C-S-H gel has a very high specific surface area, which is favourable for the adsorption and co-sedimentation of  $\text{Pb}^{2+}$ , and with the progress of the hydration reaction,  $\text{Pb}^{2+}$  can be further wrapped and immobilized during the formation of the C-S-H network structure (Chen et al., 2009). The C-S-H gel products of the MAS also gradually increased, and many needle-like Aft crystals were interspersed in the C-S-H gel, but the hydration products have significantly larger voids and a moderate degree of hydration. Macroscopically, the compressive strength was low, and the curing effect of  $\text{Pb}^{2+}$  was weak.

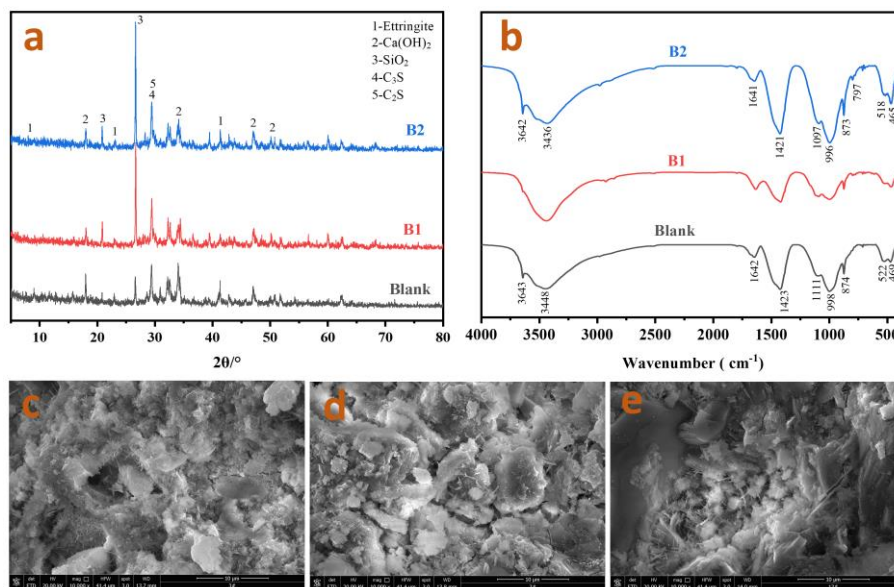


Fig. 8. Analysis of hydration products of different tungsten tailings cement system solidified bodies mixed with  $\text{Pb}^{2+}$  for 28d. (a-XRD of the solidified body; b-FT-IR of the solidified body; c-e are the SEM images of the solidified body of Blank, B1 and B2; Blank-PCS, B1-MAS, B2-TCAS)

Fig. 9 shows the analysis of the hydration products of solidified body of the TCAS with different  $\text{Pb}^{2+}$  contents. With the increase of the content of  $\text{Pb}^{2+}$  in the solidified body, the intensity of the  $\text{Ca}(\text{OH})_2$  diffraction peak of 3d was significantly weakened. The stretching vibration peak of the O-H bond contained in  $\text{Ca}(\text{OH})_2$  weakened with the increase of  $\text{Pb}^{2+}$  concentration and gradually shifted to a low wave number. This is because  $\text{Pb}^{2+}$  will first react with  $\text{OH}^-$  in the hydration environment to form  $\text{Pb}(\text{OH})_2$  precipitation, which weakens the alkaline environment in the hydration process and hinders the progress of the hydration reaction, resulting in a significant reduction in the content of  $\text{Ca}(\text{OH})_2$  in the early stage. The characteristic peak of  $\text{CaCO}_3$  was at  $1419 \text{ cm}^{-1}$  (Mollah et al., 2000), which was caused by the carbonization of  $\text{Ca}(\text{OH})_2$  during the hydration process, and it gradually migrated to a low wave number with the increase of  $\text{Pb}^{2+}$  content. The more  $\text{Pb}^{2+}$  was added, the less  $\text{CaCO}_3$  content was, which was consistent with the decrease of  $\text{Ca}(\text{OH})_2$  content. The vibrational peaks of Si-O at  $996 \text{ cm}^{-1}$  and  $876 \text{ cm}^{-1}$  (Hu et al., 2020) weakened significantly with the increase of  $\text{Pb}^{2+}$  content at 28 d, and shifted to lower wave numbers, indicating that the degree of polymerization of C-S-H gels decreased. As shown in the SEM image, with the incorporation of  $\text{Pb}^{2+}$ , the voids between the hydration product particles gradually increased, and the compactness decreased, leading to the reduction of the compressive strength of the solidified body, which was consistent with the results in Fig. 6.

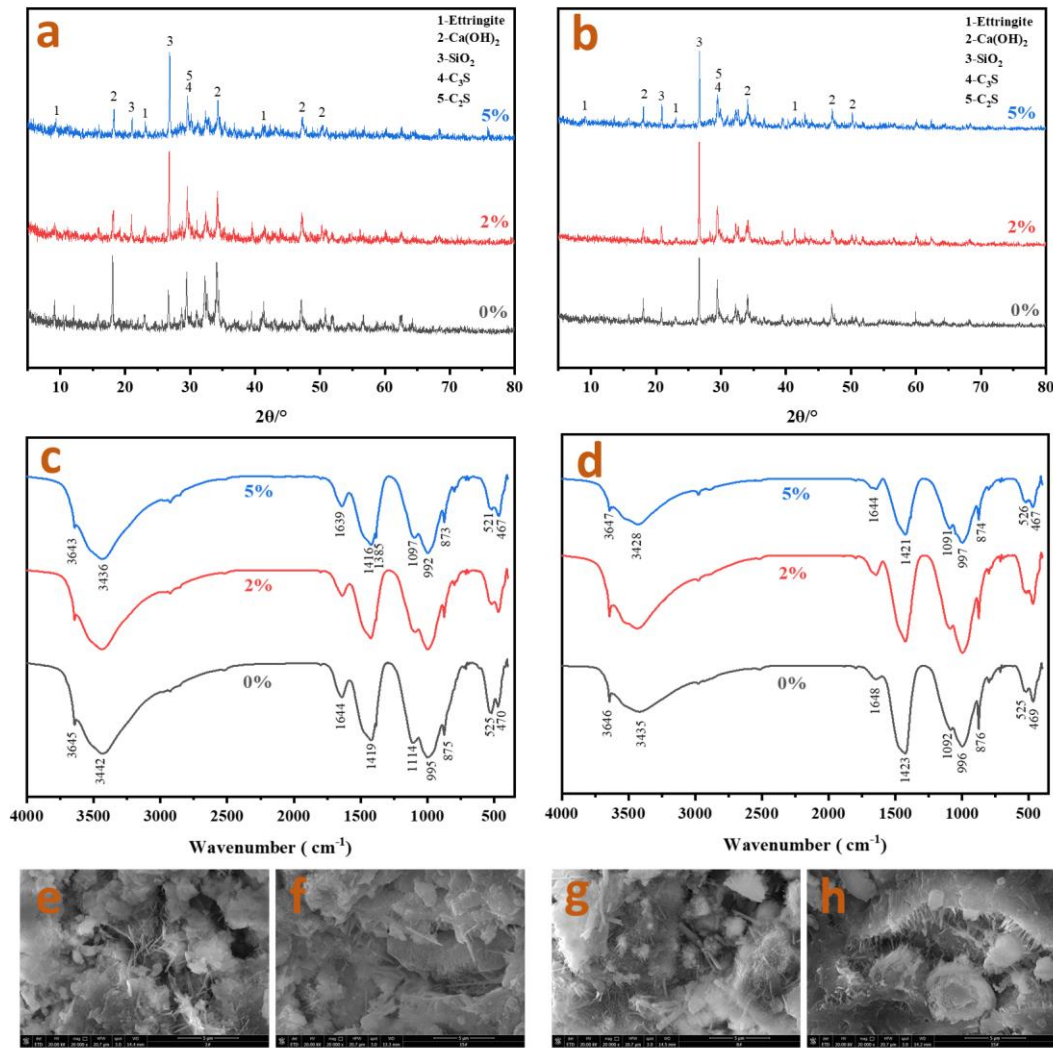


Fig. 9. Analysis of the content of  $\text{Pb}^{2+}$  on the hydration products of the solidified body of the TCAS (a, b-3d, 28d XRD; c, d-3d, 28d FT-IR; e, f-3d SEM images of  $\text{Pb}^{2+}$  content of 0% and 5%; g, h-28d SEM images of  $\text{Pb}^{2+}$  content of 0% and 5%)

Fig. 10 shows the EDS semi-quantitative analysis of the hydration products of the solidified body curing for 28d of the TCAS with  $\text{Pb}^{2+}$  content of 0, 2%, and 5%. For the slurries without  $\text{Pb}^{2+}$ , no Pb was detected in the hydration products. In Fig. 10(b), there was a bright part in the dense backscattered image of the region, and the EDS energy spectrum analysis of this region showed that O, Ca, Si, Al and Pb were contained in point 1, which indicated that there was Pb in the hydration product. Pb could be detected in the two bright areas in Fig. 10(c), and the element content reached 18.62% and 22.53%, respectively. According to the element content of the EDS spectrum and the composition of the hydration product, it is known that the hydration product is a C-S-H gel, so it can be judged that  $\text{Pb}^{2+}$  is mainly immobilized in the C-S-H gel. It may be that Pb replaces Ca in C-S-H gel, and combines with Ca and Si, so as to be fixed in C-S-H gel; it is also possible that Pb attached to the particle surface is wrapped by the newly generated C-S-H gel (Chen et al., 2009), in order to achieve the purpose of curing.

#### 4. Conclusions

Tungsten tailings have certain gelling activity after activation. There are different effects in the treatment of tailings by different activation methods. After ternary composite activation, the particle size distribution of tailings can be effectively changed, and the specific surface area of tailings particles can be increased, which is better than other activation conditions. It can participate in the hydration reaction

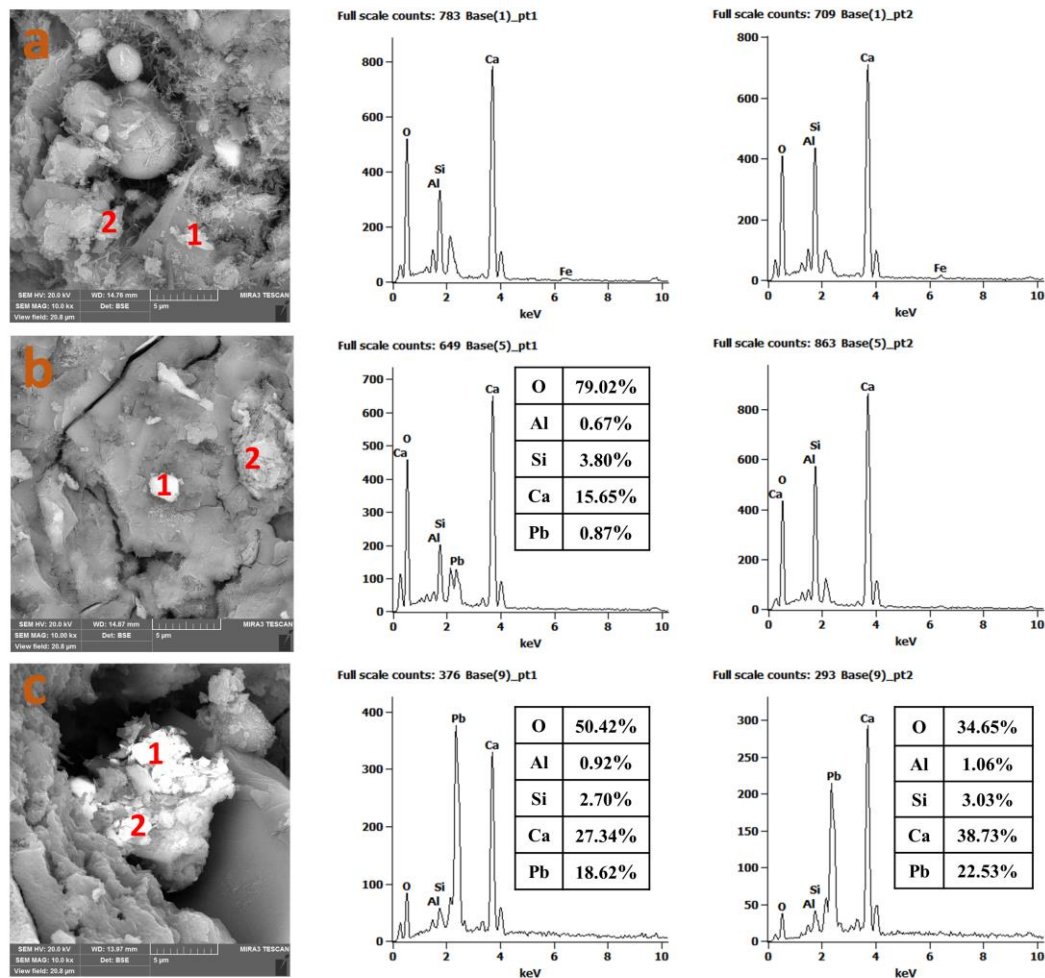


Fig. 10. EDS analysis of hydration products of the TCAS (a-0%Pb, b-2%Pb, c-5%Pb) of the cement system, the compressive strength of the solidified body formed with the cement is the best, and the effect of preventing  $Pb^{2+}$  leaching is the best

The content of  $Pb^{2+}$  and the curing age will affect the curing effect. Under standard curing conditions, with the increase of the content of  $Pb^{2+}$  in the solidified body, the leaching rate of  $Pb^{2+}$  gradually increased, and the compressive strength decreased; with the extension of curing age, the leaching rate of  $Pb^{2+}$  gradually decreased, and the compressive strength of the solidified body increased. When the mass fraction of  $Pb^{2+}$  was 5%, the leaching rate of  $Pb^{2+}$  of PCS for 28d was only 0.0240%, that of TCAS was 0.0253%, the  $Pb^{2+}$  leaching concentration of TCAS was only 0.38 mg/L, which was within the safety limit specified in Chinese standard (GB5085.3-2007). Therefore, tungsten tailings synergize with cement to solidify  $Pb^{2+}$  is a green way to realize the resource utilization of tailings and treatment of the lead-containing wastewater.

$Pb^{2+}$  can be effectively immobilized in the hydration product C-S-H gel of the solidified body. In addition to the C-S-H gel generated by cement hydration, the active  $SiO_2$  in the solidified body tailings have a pozzolanic reaction with the  $Ca(OH)_2$  generated by cement hydration. The Si-O bond breaks, recombines, then polymerizes into Si-O-Si bond, and eventually forms a structurally stable C-S-H gel. According to the analysis of SEM and EDS,  $Pb^{2+}$  can be effectively immobilized in the "calcium-silicon-rich" hydration product C-S-H gel. It may be that Pb replaces Ca in C-S-H gel, it is also possible that Pb attached to the particle surface is wrapped by the newly generated C-S-H gel.

### Acknowledgments

Thanks for the financial assistance from the National Key Research and Development Program of China (No. 2018YFC1903403).

## References

- ALFONSO, P., TOMASA, O., GARCIA-VALLES, M., TARRAGO, M., MARTINEZ, S., ESTEVES, H., 2018. *Potential of tungsten tailings as glass raw materials*. Mater. Lett. 228, 456-458.
- CHEN, Q.Y., TYRER, M., HILLS, C.D., YANG, X.M., CAREY, P., 2009. *Immobilisation of heavy metal in cement-based solidification/stabilisation: A review*. Waste Manage. 29(1), 390-403.
- CHEN, D.N., LI, D.G., Z.J., XIAO, FANG, Z., ZOU, X.G., CHEN, P., CHEN, T.S., LV, W.Y., LIU, H.J., LIU, G.G., 2021. *Removal of lead ions by two Fe-Mn oxide substrate adsorbents*. Sci. Total Environ. 773, 145670.
- CHOI, Y.W., KIM, Y.J., CHOI, O., LEE, K.M., LACHEMI, M., 2009. *Utilization of tailings from Tungsten mine waste as a substitution material for cement*. Constr. Build. Mater. 23(7), 2481-2486.
- CONNER, J.R., HOEFFNER, S.L., 1998. *A critical review of stabilization/solidification technology*. Crit. Rev. Env. Sci. Tec. 28(4), 397-462.
- EI-ESWED, B.I., ALDAGAG, O.M., KHALILI, F.I., 2017. *Efficiency and mechanism of stabilization/solidification of Pb(II), Cd(II), Cu(II), Th(IV) and U(VI) in metakaolin based geopolymers*. Appl. Clay Sci. 140, 148-156.
- EL-ESWED, B.I., 2020. *Chemical evaluation of immobilization of wastes containing Pb, Cd, Cu and Zn in alkali-activated materials: A critical review*. J. Environ. Chem. Eng. 8(5), 104194.
- FENG, C.Y., ZENG, Z.L., ZHANG, D.Q., QU, W.J., DU, A.D., LI, D.X., SHE, H.Q., 2011. *SHRIMP zircon U-Pb and molybdenite Re-Os isotopic dating of the tungsten deposits in the Tianmenshan-Hongtaoling W-Sn orefield, southern Jiangxi Province, China, and geological implications*. Ore Geol. Rev. 43(1), 8-25.
- FENG, Y., QI, J.Y., CHI, L.Y., WANG, D., WANG, Z.Y., LI, K., LI, X., 2013. *Production of sorption functional media (SFM) from clinoptilolite tailings and its performance investigation in a biological aerated filter (BAF) reactor*. J. Hazard. Mater. 246-247, 61-69.
- GLASSER, F. P., 1997. *Fundamental aspects of cement solidification and stabilization*. J. Hazard. Mater. 52(2-3):151-170.
- HALIM, C.E., AMAL, R., BEYDOUN, D., SCOTT, J.A., LOW, G., 2004. *Implications of the structure of cementitious wastes containing Pb(II), Cd(II), As(V), and Cr(VI) on the leaching of metals*. Cement Concrete Res. 34(7), 1093-1102.
- HU, S.X., ZHONG, L.L., YANG, X.J., BAI, H.Y., REN, B., ZHAO, Y.L., ZHANG, W., JU, X., WEN, H.R., MAO, S.R., TAO, R., LI, C., 2020. *Synthesis of rare earth tailing-based geopolymer for efficiently immobilizing heavy metals*. Constr. Build. Mater. 254, 119273.
- HUANG, J.L., LUO, Z.B., KHAN, M.B.E., 2020. *Impact of aggregate type and size and mineral admixtures on the properties of pervious concrete: An experimental investigation*. Constr. Build. Mater. 265, 120759.
- HUANG, Z.Q., ZHANG, S.Y., WANG, H.L., LIU, R.K., CHENG, C., SHUAI, S.Y., HU, Y.J., ZENG, Y.H., YU, X.Y., HE, G.C., FU, W., BUROV, V.E., POILOV, V.Z., 2022. *Recovery of wolframite from tungsten mine tailings by the combination of shaking table and flotation with a novel "crab" structure sebacoil hydroxamic acid*. J. Environ. Manage. 317, 115372.
- JI, Z.H., PEI, Y.S., 2019. *Bibliographic and visualized analysis of geopolymer research and its application in heavy metal immobilization: A review*. J. Environ. Manage. 231, 256-267.
- JI, Z.H., PEI, Y.S., 2020. *Immobilization efficiency and mechanism of metal cations (Cd<sup>2+</sup>, Pb<sup>2+</sup> and Zn<sup>2+</sup>) and anions (AsO<sub>4</sub><sup>3-</sup> and Cr<sub>2</sub>O<sub>7</sub><sup>2-</sup>) in wastes-based geopolymer*. J. Hazard. Mater. 384, 121290.
- JI, G.X., PENG, X.Q., WANG, S.P., HU, C., RAN, P., SUN, K.K., ZENG, L., 2021. *Influence of magnesium slag as a mineral admixture on the performance of concrete*. Constr. Build. Mater. 295, 123619.
- KATSOU, E., MALAMIS, S., HARALAMBOUS, K., 2011. *Pre-treatment of industrial wastewater polluted with lead using adsorbents and ultrafiltration or microfiltration membranes*. Water Environ. Res. 83(4), 298-312.
- KHAN, A.H., SHANG, J.Q., ALAM, R., 2012. *Ultrasound-assisted extraction for total sulphur measurement in mine tailings*. J. Hazard. Mater. 235-236, 376-383.
- KHARRAZ, J.A., KHANZADA, N.K., FARID, M.U., KIM, J., JEONG, S., AN, A.K., 2022. *Membrane distillation bioreactor (MDBR) for wastewater treatment, water reuse, and resource recovery: A review*. J. Water Process Eng. 47, 102687.
- KOROGLU, L., KAMAN, D.O., AYAS, E., 2021. *Optimizing the particle size distribution of heat-treated boron derivative wastes in cement mortars as portland cement replacements*. Constr. Build. Mater. 282, 122640.
- KUMAR, M., NANDI, M., PAKSHIRAJAN, K., 2021. *Recent advances in heavy metal recovery from wastewater by biogenic sulfide precipitation*. J. Environ. Manage. 278, 111555.
- LEE, D., 2007. *Formation of leadhillite and calcium lead silicate hydrate (C-Pb-S-H) in the solidification/stabilization of lead contaminants*. Chemosphere. 66(9), 1727-1733.

- LEE, P.K., KANG, M.J., JO, H.Y., CHOI, S.H., 2012. *Sequential extraction and leaching characteristics of heavy metals in abandoned tungsten mine tailings sediments*. Environ. Earth Sci, 66, 1909-1923.
- LEE, J. K., SHANG, J.Q., JEONG, S., 2014. *Thermo-mechanical properties and microfabric of fly ash-stabilized gold tailings*. J. Hazard. Mater. 276, 323-331.
- LIU, C.P., LUO, C.L., GAO, Y., LI, F.B., LIN, L.W., WU, C.A., LI, X.D., 2010. *Arsenic contamination and potential health risk implications at an abandoned tungsten mine, southern China*. Environ. Pollut. 158(3), 820-826.
- LIU, X.M., SONG, Q.J., TANG, Y., LI, W.L., XU, J.M., WU, J.J., WANG, F., BROOKES, P.C., 2013. *Human health risk assessment of heavy metals in soil-vegetable system: A multi-medium analysis*. Sci. Total Environ. 463-464, 530-540.
- MOLLAH, M.Y.A., YU, W.H., SCHENNACH, R., COCKE, D.L., 2000. *A Fourier transform infrared spectroscopic investigation of the early hydration of Portland cement and the influence of sodium lignosulfonate*. Cement Concrete Res. 30(2), 267-273.
- MONTEIRO, P.J.M., MILLER, S.A., HORVATH, A., 2017. *Towards sustainable concrete*. Nat. Mater. 16(7), 698-699.
- OLIVEIRA DE SOUZA, P., SINHOR, V., CRIZEL, M.G., PIRES, N., FILHO, P.J.S., PICOLOTO, R.S., DUARTE, F.A., PEREIRA, C.M.P., MESKO, M.F., 2022. *Bioremediation of chromium and lead in wastewater from chemistry laboratories promotes by cyanobacteria*. Bioresource Technology Reports, 19, 101161.
- PENG, J.T., ZHOU, M.F., HU, R.Z., SHEN, N.P., YUAN, S.D., BI, X.W., DU, A.D., QU, W.J., 2006. *Precise molybdenite Re-Os and mica Ar-Ar dating of the Mesozoic Yaogangxian tungsten deposit, central Nanling district, South China*. Miner. Deposita. 41(7), 661-669.
- PENG, K., YANG, H.M., OUYANG, J., 2015. *Tungsten tailing powders activated for use as cementitious material*. Powder Technol. 286, 678-683,
- PETRUNIC, B.M., AL, T.A., WEAVER L., 2006. *A transmission electron microscopy analysis of secondary minerals formed in tungsten-mine tailings with an emphasis on arsenopyrite oxidation*. Appl. Geochem. 21(8), 1259-1273.
- PRANUDTA, A., CHANTHAPON, N., KIDKHUNTHOD, P., EL-MOSELHY, M.M., NGUYEN, T.T., PADUNGTHON, S., 2021. *Selective removal of Pb from lead-acid battery wastewater using hybrid gel cation exchanger loaded with hydrated iron oxide nanoparticles: Fabrication, characterization, and pilot-scale validation*. J. Environ. Chem. Eng. 9(5),106282.
- RAVISHANKAR, H., MOAZZEM, S., JEGATHEESAN, V., 2019. *Performance evaluation of A2O MBR system with graphene oxide (GO) blended polysulfone (PSf) composite membrane for treatment of high strength synthetic wastewater containing lead*. Chemosphere. 234, 148-161.
- SIDDIQUE R., 2010. *Utilization of municipal solid waste (MSW) ash in cement and mortar*. Resour. Conserv. Recy. 54(12), 1037-1047.
- TIAN, Y.X., THEMELIS, N.J., ZHAO, D.D., BOURTSALAS, A.C.T., KAWASHIMA, S., 2022. *Stabilization of Waste-to-Energy (WTE) fly ash for disposal in landfills or use as cement substitute*. Waste Manage. 150, 227-243.
- WANG, X., QIN, W.Q., JIAO, F., DONG, L.Y., GUO, J.G., ZHANG, J., YANG, C.R., 2022. *Review of tungsten resource reserves, tungsten concentrate production and tungsten beneficiation technology in China*. T. Nonferr. Metal. Soc. 32, (7), 2318-2338.
- WHITWORTH, A.J., VAUGHAN, J., SOUTHAM, G., ENT, A., NKRUMAH, P.N., MA, X.D., PARBHAKAR-FOX, A., 2022. *Review on metal extraction technologies suitable for critical metal recovery from mining and processing wastes*. Miner. Eng. 182, 107537.
- WU, Z.X., JIANG, Y.M., GUO, W.X., JIN, J.X., WU, M.J., SHEN, D.S., LONG, Y.Y., 2021. *The long-term performance of concrete amended with municipal sewage sludge incineration ash*. Environ. Technol. Inno. 23, 101574.
- YUAN, W.Q., KUANG, J.Z., YU, M.M., HUANG, Z.Y., ZOU, Z.L., ZHU, L.P., 2021. *Facile preparation of MoS<sub>2</sub>@Kaolin composite by one-step hydrothermal method for efficient removal of Pb(II)*. J. Hazard. Mater. 405, 124261.
- ZHU, Y., GUO, B., ZUO, W.R., JIANG, K.X., CHEN, H.H., KU, J.G., 2022. *Effect of sintering temperature on structure and properties of porous ceramics from tungsten ore tailings*. Mater. Chem. Phys. 287, 126315.